

Coupling dark-baryonic matter density profile for vacuum decay scenarios*

H. T. C. M. Souza

*Universidade Federal Rural do Semi-Árido - DECEN, Brazil and
Universidade Federal do Rio Grande do Norte - DFTE, Brazil*[†]

N. Pires[‡]

Universidade Federal do Rio Grande do Norte - DFTE, Brazil[†]

F. E. M. Costa[§]

Universidade Federal Rural do Semi-Árido - DECEN, Brazil

F. C. Carvalho[¶] and E. P. Bento^{**}

Universidade do Estado do Rio Grande do Norte - DF, Brazil

(Dated: April 18, 2022)

The cosmological consequences of an interacting model in which vacuum decay law is deduced from the effect that vacuum decay has on the dark matter evolution are investigated. Here, the baryonic matter is also considered as a fluid gravitationally coupled with dark matter. It is made a careful analysis to constrain this model with the observational data of growth rate of cosmic structures. The theoretical growth rate is followed since the primordial recombination and the main physical processes on the baryonic component are considered. As a complementary constraint, this model is compared with the observed CMB-BAO ratio as well with the gas mass fraction of cluster of galaxies. We found the best fit values for dark matter $\Omega_{d0} = 0.269^{+0.023}_{-0.023}$ and for the decay parameter $\epsilon = 0.02^{+0.04}_{-0.05}$.

Keywords: Spherical Top-Hat collapse, linear growth rate, cooling function, vacuum decay model.

I. INTRODUCTION

Several astronomical observations (Supernova Ia distance, age of the universe estimates, measurements of the cosmic microwave background radiation anisotropies etc.) have convergently indicated that the universe is undergoing by a recent accelerated expansion. In the context of the General Relativity, this has been attributed to an exotic component of energy with negative pressure, which is the so called dark energy (see a pedagogical review in [1]).

The nature and origin of this dark component is still a completely open question. Among several candidates for dark energy, the oldest and most natural is the cosmological constant Λ [2], interpreted as the vacuum energy, i.e., $\rho_\Lambda = \Lambda/8\pi G$. Moreover, here we face with the cosmological constant problem which is the conflict between the upper cosmological limit today ($\rho_\Lambda \sim 10^{-47} GeV^4$), and the theoretical expectation within the framework of the quantum field theory ($\sim 10^{71} GeV^4$) for the vacuum energy value. In this regard, a phenomenological attempt to alleviate such problem is allowing Λ to vary with time. Even before the discovery of the accelerating expansion, many works had been already dedicated

in the time-evolving vacuum models. These models were motivated in the attempt to explain the cosmological constant problem as well as the age of the universe [3]. With the discovery of the accelerated expansion the interest in them increase, because they can explain the accelerated expansion of the universe in an efficient way, and also provide an interesting attempt to evade the coincidence and cosmological constant problems of the standard Λ -cosmology ([4], and also for a more complete history see [5]).

An interesting and more realistic approach based on the modified matter expansion rate was proposed by Wang & Meng [6]. Afterwards, in this model, Alcaniz & Lima [7] included the baryonic component and showed that its presence changes the dynamic of the evolution altering the transition redshift for values compatible with current estimates based on type Ia supernova.

The aim of the present paper is to investigate the cosmology of the vacuum decaying into cold dark matter (CDM), proposed in [6], considering the growth rate of matter (dark and baryonic) since the recombination era taking into account the main physical mechanisms in the baryonic component, through the exact calculations of the hydrodynamical equations. The physical processes that we take into account are photon drag, photon cooling, recombination, photoionization, collisional ionization, and hydrogen molecule production, destruction and cooling - hereafter called simply ‘physical mechanisms’. Baryonic and dark matter are considered as two fluids coupled only by gravity.

The outline of our paper is as follows. In section II is

* A footnote to the article title

[†] hidalyn.souza@ufersa.edu.br

[‡] npires@dfte.ufrn.br

[§] ernandesmatos@ufersa.edu.br

[¶] fabiocabral@uern.br

** eliangela@dfte.ufrn.br

briefly described the vacuum decay model. Our model of dark and baryonic contrast and the growth rate in framework proposed by [6] are presented in section III, as well the constraint with the observational data of growth rate of cosmological structures. As an additional constraint for the vacuum decay model are done two complementary observation tests: ‘‘CMB-BAO’’ and ‘‘Gas mass fraction of galaxy clusters’’, presented in section IV. The conclusions are presented in section V, and in appendix A is showed the calculations of the temporal evolution of the baryonic matter.

II. VACUUM DECAY MODEL

Let us first consider a homogeneous and isotropic universe described by the Friedmann-Lemaitre-Robertson-Walker element line and a coupling between Λ and CDM particles. In this case, we have that

$$\dot{\rho}_d + 3\frac{\dot{a}}{a}\rho_d = -\dot{\rho}_\Lambda, \quad (1)$$

where ρ_d and ρ_Λ are the energy densities of CDM and Λ , respectively, a is the cosmic scale factor and the dot sign denotes derivative with respect to the time.

In the traditional approach, the description of the cosmological scenario with a dynamical Λ term there is the necessity of specify a phenomenological time dependent law for the vacuum. However, Ref. [6] (see also [7]) found a decay law is deduced from the effect that vacuum has on the dark matter evolution.

The qualitative argument used in Ref. [6] is the following: if vacuum is decaying into CDM particles, the energy density of this latter component will dilute more slowly compared to its standard evolution $\rho_d \propto a^{-3}$. Thus, the deviation from the standard dilution is characterized by a positive constant, such that

$$\rho_d = \rho_{d0} a^{-3+\epsilon}, \quad (2)$$

where ρ_{d0} is the current value of ρ_d (for the remainder of this and the next sections, all quantities with subscript zero will imply that we are considering the current value).

Now, by substituting the ansatz (2) in Eq. (1) yields the vacuum energy density

$$\rho_v = \tilde{\rho}_{v0} + \frac{\epsilon\rho_{d0}}{3-\epsilon} a^{-3+\epsilon}, \quad (3)$$

where $\tilde{\rho}_{v0}$ is an integration constant which represents the ‘ground state value of the vacuum’, i.e., the standard vacuum energy density. Notice that when $\epsilon = 0$ the standard Λ CDM model is recovered.

Neglecting the radiation contribution and considering that the baryonic content is separately conserved, the expansion rate of the Universe can be written as

$$H = H_0 \left[\Omega_{b0} a^{-3} + \frac{3\Omega_{d0}}{3-\epsilon} a^{-3+\epsilon} + \tilde{\Omega}_{v0} \right]^{1/2}, \quad (4)$$

where $\Omega_{b0} = \rho_{b0}/\rho_{c0}$ and $\Omega_{d0} = \rho_{d0}/\rho_{c0}$ represent the density parameters of baryons and dark matter, while that $\Omega_{v0} = \tilde{\rho}_{v0}/\rho_{c0}$ the density parameter associated to constant $\tilde{\rho}_{v0}$. From normalization condition, one has

$$\tilde{\Omega}_{v0} = 1 - \Omega_{b0} - \frac{3\Omega_{d0}}{3-\epsilon}. \quad (5)$$

The term Ω_{b0} in Eq. (4), separately conserved, was included by Ref. [7], which showed that baryonic contribution cannot be neglected because it reconciles the decaying vacuum scenario with the observations. Besides, in the present work we are also taking into account the physical mechanisms in this component.

As pointed in reference [7], an important restriction on ϵ value given by second law of Thermodynamics implies that $\epsilon \geq 0$ and also $\epsilon \leq 1$ (or even should expect $\epsilon \ll 1$ due to no observational report anomalous on the CDM expansion rate yet), which avoid the accelerated phase of the universe has begun in the matter-dominated era [6]. The analysis of the growth of perturbations can also provide one important restriction on the $\Lambda(t)$ CDM models. The presence of a dynamical vacuum energy provides a critical value to the decay parameter from which fluctuations do not collapse ($\epsilon > 0.4$), no matter its size in the recombination. These aspects will be considerably important because they provide an initial constraint when we will do the comparison with the observational data.

III. COSMOLOGICAL CONSTRAINT: GROWTH RATE OF COSMIC STRUCTURE

As we are focusing the importance of the attractive matter components, becomes interesting to compare this decaying model with the data set related with matter. In order to do this we compare our model with the observational growth factor (see table I).

To constrain the parametric space $\Omega_{d0} - \epsilon$, we use the χ^2 minimization

$$\chi_{gf}^2 = \sum_{i=1}^{10} \left(\frac{f(z_i)_{obs} - f(z_i, \theta_i)_{th}}{\sigma_{gfi}} \right)^2, \quad (6)$$

where $f(z_i)_{th}$ is the theoretical value of the growth factor given by equation (15) (bellow), $f(z_i)_{obs}$ is the observational data shown in table I and σ_{gfi} is the error of the $f(z_i)_{obs}$.

In the following, we present our theoretical model for the growth rate of the structures.

There is a tight connection between cold collisionless dark matter and baryonic matter. Furthermore, there are several physical mechanisms occurring in the baryonic matter which lack for dark matter during its evolution. The density contrast in these components were modelled as a cloud that contains a certain dark matter mass M_d of radius r_d , and we follow only the baryonic matter that is inside this cloud. As described in

z	f_{obs}	Ref.
0.02	0.48 ± 0.09	[30]
0.07	0.56 ± 0.11	[31]
0.15	0.51 ± 0.11	[29]
0.22	0.60 ± 0.10	[32]
0.34	0.64 ± 0.09	[33]
0.35	0.70 ± 0.08	[34]
0.41	0.70 ± 0.07	[32]
0.42	0.73 ± 0.09	[35]
0.59	0.75 ± 0.09	[35]
0.60	0.73 ± 0.07	[32]
0.78	0.70 ± 0.08	[32]

TABLE I. Observational values of the linear growth rate. In the first column is the sample redshift, the second one shows the growth rate value in the redshift and the corresponding central error bar (standard deviation) and, finally, in the third column the references related to each measurement.

appendix A, the physical processes considered here are the photon cooling (heating), collisional ionization, photoionization, Lyman- α cooling, and the cooling due to H_2 formation. In order to evolve the matter fluctuation (or cloud), it was considered as having a ‘top-hat’ profile as proposed in reference [37].

The baryonic matter and dark matter are considered as two fluids coupled only by gravity. As their evolution is non-relativistic, Newtonian hydrodynamic equations is used to describe them. The contrast densities for baryonic, δ_b , and dark matter, δ_d , are defined as usually,

$$\delta_b = \frac{\delta\rho_b}{\rho_b} \quad \text{and} \quad \delta_d = \frac{\delta\rho_d}{\rho_d}. \quad (7)$$

Considering the top-hat model, the perturbation has a square density profile and a linear dependence for the velocity (which is consistent with the density profile)

$$\rho_{ci} = \rho_i + \rho_{1i}(t) = \rho_i[1 + \delta_i(t)] \quad (8a)$$

$$\mathbf{v}_{ci} = H\mathbf{r} + v_{1i}(t)\frac{\mathbf{r}}{r_i}, \quad (8b)$$

where the subscript i means baryonic or dark matter, r_i the radius of the clouds components, $\rho_{1i}(t)$ is the perturbation, $v_{1i}(t)$ is the peculiar velocity of the fluctuation, $\delta_i(t)$ is the density contrast of the perturbation, and \mathbf{r} is the radial coordinate centered in the cloud.

The collapse of a cloud with two components coupled initially begins with a cloud of dark and baryonic matter. As the collapse continues, the dark cloud collapses faster than the baryonic one, which is delayed by the physical mechanisms acting on it. Thus, part of the initial baryonic matter is left behind and we follow only that goes with the dark matter, i.e., $M_b(t)$. The surrounding medium forms a halo that could eventually interact with the cloud that is collapsing. As both baryonic and dark matter are into the same volume over time, the amount of baryonic matter M_d related to the mass of dark matter M_a shall be given by

$$M_b(a) = M_d \frac{\Omega_{b0}}{\Omega_{d0}} \left(\frac{1 + \delta_b}{1 + \delta_d} \right) a^{-\epsilon}. \quad (9)$$

The hydrodynamics equations are (see [37] and [11]) the continuity equation,

$$\frac{\partial\rho_{ci}}{\partial t} + \nabla \cdot (\rho_{ci}\mathbf{v}_{ci}) = 0, \quad (10)$$

the motion equation,

$$\frac{d\mathbf{v}_{ci}}{dt} + (\mathbf{v}_{ci} \cdot \nabla)\mathbf{v}_{ci} = -\nabla\phi - \frac{1}{\rho_{ci}}\nabla P - \frac{4}{3}\frac{\sigma_T b T_\gamma^4 x_e}{m_p c}(\mathbf{v}_{ci} - H\mathbf{r}), \quad (11)$$

where P is the pressure, σ is the Thomson cross section, $b = 4/c$ is the Stefan-Boltzmann’s constant, x_e is the degree of ionization, and the last term is the photon drag due to the background radiation; and the field equation itself is

$$\nabla^2\phi = 4\pi G\rho_{ci}. \quad (12)$$

Note that for the dark matter component the two last terms in equation (11) do not exist (dark particles are collisionless and do not interact with photons).

Substituting the perturbations (7) in the subsequent equations (8) - (12) we obtain the density contrast of dark matter at any time,

$$\dot{\delta}_d + 3(1 + \delta_d)\frac{v_{1d}}{r_d} = 0, \quad (13a)$$

and the velocity of the dark cloud

$$v_{1d} + H v_{1d} + \frac{4\pi G\rho_{oc} r_d}{3} a^{-3} [\Omega_{b0} + \Omega_{d0} a^\epsilon] (\delta_b + \delta_d) = 0; \quad (13b)$$

as well the evolution of the density contrast of the baryonic matter

$$\dot{\delta}_b + 3(1 + \delta_b)\frac{v_{1b}}{r_b} = 0, \quad (14a)$$

and the velocity of baryonic cloud inside the dark cloud (which follows the dark cloud),

$$v_{1b} + v_{1b} \left(H + \frac{4}{3} \frac{\sigma_T b T_\gamma^4 x_e}{m_p c} \right) + \frac{4}{3} \pi G r_b \rho_{c0} a^{-3} [\Omega_{b0} + \Omega_{d0} a^\epsilon] \cdot (\delta_b + \delta_d) - \frac{N_A k_B}{r_d} T_m (1 + x_e) = 0. \quad (14b)$$

Here, T_m is the temperature of the baryonic matter, which has its dependence over time calculated in appendix A, m_p is the mass of proton and, just remembering, ϵ is the parameter of the vacuum decay.

According to equation (8b), in the linear approximation the velocity of the fluctuations can be resolved into a term which tells us about the expansion of the universe, $H\mathbf{r}$, and also another representing the peculiar velocity of the cloud, as suggested by Peebles [8], $\mathbf{u}(t) = v_{1i}(t)\mathbf{r}/r_i = 2/3[f(z)\mathbf{g}(\mathbf{r})/(H(z)\Omega_m(z))]$. In this expression $\mathbf{g}(\mathbf{r})$ is the specific gravity of the cloud and $f(z)$ is the linear growth rate, which is related with the

growth mode of the perturbation of the baryonic and dark matter components as

$$f = \frac{a}{\delta} \frac{d\delta}{da} = \frac{\dot{\delta}_b + \dot{\delta}_d}{\delta_b + \delta_d} . \quad (15)$$

Originally, in 1980 Peebles found $f(z=0) = \Omega_{m0}^{0.6}$ [8], a quite useful approximation of the linear growth rate obtained from the Friedmann-Lemaître model, valid for cases where the cosmological constant or curvature of space can be neglected [9]. Afterwards, more accurate approximations for this same model were found, as for instance, $f(z=0) = \Omega_{m0}^{4/7}$ by Lightman & Schechter [10]. Later, other analysis were performed taking into account the cosmological constant and the variation of the growth rate with the redshift (for a brief review see for example [11]). For a flat universe with cosmological constant, a very useful utilized approximation was found by Lahav et al. [12]

$$f(z) = \Omega'_m{}^{0.6} + \frac{1}{70} \left[1 - \frac{\Omega'_m}{2} (1 + \Omega'_m) \right] . \quad (16)$$

where

$$\Omega'_m(z) \equiv \frac{\Omega_{b0} a^{-3} + \Omega_{d0} a^{-3+\epsilon}}{\Omega_{b0} a^{-3} + \Omega_{d0} a^{-3+\epsilon} + \Omega_{v0}} , \quad (17)$$

is the normalized matter density parameter. A similar approach was first made by Wang & Steinhardt [13].

Based on the results from seven-year WMAP data set (WMAP7 - [14]), we assume a spatial flat universe with density parameter values for current baryonic matter $\Omega_{b0} = 0.0458$ and dark matter $\Omega_{d0} = 0.229$, and the Hubble constant $H_0 = 70.2 \text{ km s}^{-1} \text{ Mpc}^{-1}$. As initial conditions for our numerical code the evolution of the fluctuations start when 90% of all primordial hydrogen already recombined (when the radiation temperature $T_\gamma \simeq 4000 \text{ K}$ and $z \simeq 1500$). The inputs for the initial contrast of baryonic density is $\delta_d^{rec} = 0$ (because we do not expect any initial fluctuation of baryonic matter at this time due to its recently tight interaction with the CMB photons) and $\delta_d^{rec} = 10^{-5}$ (after matter radiation equality, dark matter fluctuations grew little and we supposed that they are not much bigger than that of the CMB). The amount of dark mass of the fluctuation is also an initial input of the numerical calculation and the value that we used was $10^{14} M_\odot$, which mimics a cluster of galaxies and almost a linear fluctuation. Figure 1a shows clearly this point: fluctuations with $M_d < 10^{14} M_\odot$ fail to represent $f(z=0)$ corresponding to the observations (see table I for the observational data).

The evolution of the linear growth rate since recombination is shown in figure 1b. For the sake of comparison, the Lahav approximation from equation (16) is also plotted in the same figure (dashed curve).

The curve signed $\epsilon = 0.0$ (solid curve) coincides with the Λ CDM model, and it is quite similar to Lahav approximation (long-dashed curve), at least for $0 \leq z \lesssim$

100. The cases $\epsilon = 0.1$ and $\epsilon = 0.2$ (pointed and dashed-dot curves, respectively) follow that to $\epsilon = 0.0$, but the amplitude is smaller as bigger as the value of ϵ . This trend was already expected because in these models with decaying vacuum the density of dark matter is smaller in higher redshifts (see equation (2)). This reflects what is shown in figure 3 of the evolution of the total density contrast. Note that, all the models showed in this figure has its present growth rate value (i.e., $f(z=0)$) close to the observational value $\Omega_m^{0.55} = (\Omega_{b0} + \Omega_{d0})^{0.55} \simeq 0.48$ (see [10] or [19]). The second and third column of table II, give the numerically calculated values for the today values of the growth rate (respectively with and without the baryonic component) for three classes of models with $\epsilon = 0.0$ ($= \Lambda$ CDM), 0.1, and 0.2.

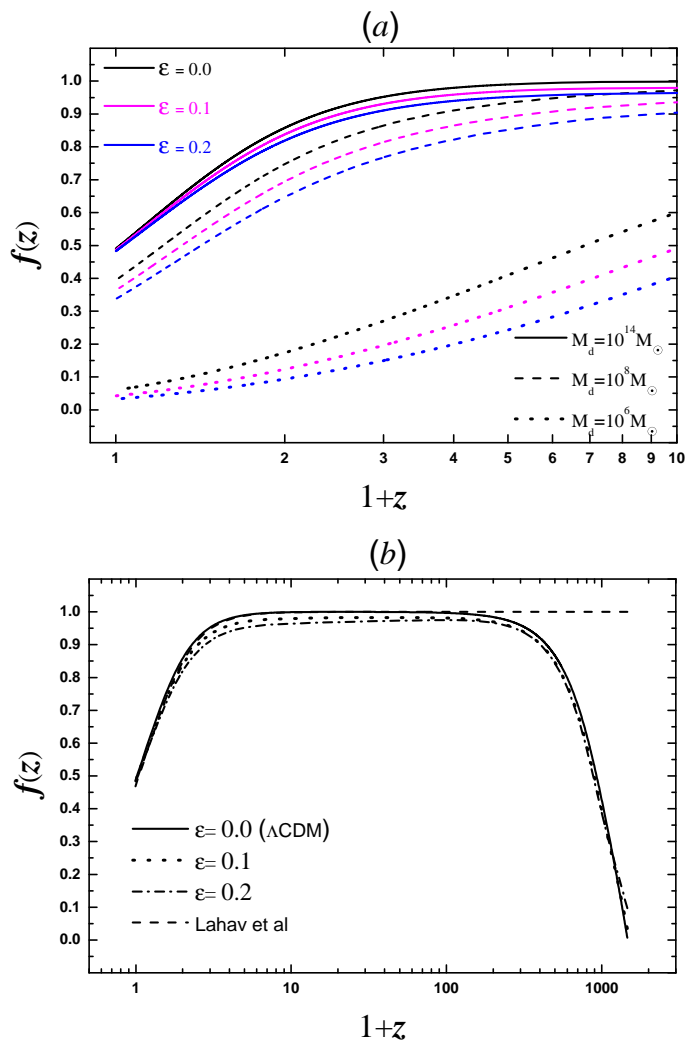


FIG. 1. (a) Numerical evolution of the linear growth rate from equation (15) for $\epsilon = 0$ ($\equiv \Lambda$ CDM), $\epsilon = 0.1$, and $\epsilon = 0.2$. Mass scales like $M_d < 10^{14} M_\odot$ seems not to represent growth rate today in correspondence to observations ($f_0 = 0.5$) [36]. (b) Evolution of the linear growth rate since the recombination era. The Lahav approximation from equation (16) is also plotted. These curves are only for $M_d = 10^{14} M_\odot$ and consider the WMAP result set $\Omega_{b0} = 0.0458$, $\Omega_{d0} = 0.229$ and $h = 0.702$ [14].

ϵ	f_0	f_0^*
0.0	0.490	0.442
0.1	0.486	0.436
0.2	0.483	0.430

* Stands for the case $\Omega_b = 0$.

TABLE II. Today values of the numerical growth rate, with and without the baryonic component, f_0 and f_0^* , respectively, for three values of the parameter ϵ . In this analysis $\Omega_{d0} = 0.229$, $\Omega_{b0} = 0.0458$, and $h = 0.702$.

Figure 2 gives the evolution of $f(z)$ in low redshifts, and shows the importance of take into account the baryonic matter.

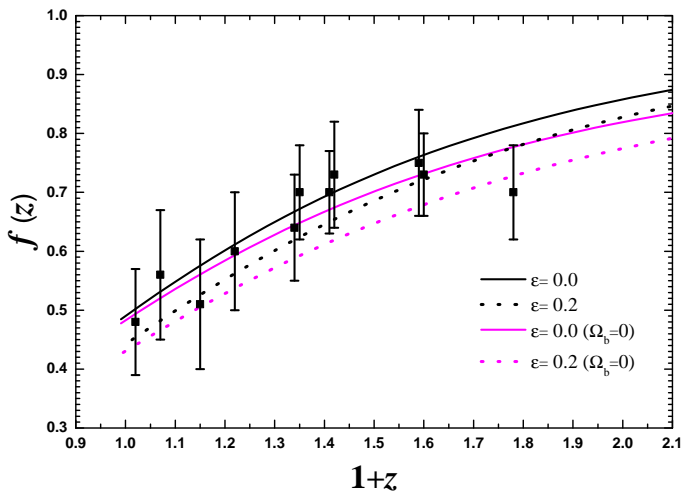


FIG. 2. The points with error bar are the observed data (see table I). This figure shows also the curves for $\epsilon = 0.0$ ($\equiv \Lambda$ CDM) and $\epsilon = 0.2$ with the inclusion of baryonic matter and without it. No significant difference from the curves with baryonic matter was found when the physical cooling/heating processes were absent.

In this figure is also superimposed the observed values of $f(z)$ and their error bars, which are tabled in table I. The theoretical curves shown that a smaller amplitude of $f(z)$ for the cases without baryonic matter. Comparing the results obtained with the observational data set, we find that these models are viable because they are within the error bars.

Figure 3 shows the evolution of the total (dark plus baryonic) density contrast for the three classes of models with $\Lambda(t)$: $\epsilon = 0.0$ ($= \Lambda$ CDM plus baryonic matter), 0.1, and 0.2. In this picture is also presented the effects of take into account dark matter and baryonic matter plus the physical mechanisms (dark curves), dark matter and baryonic matter without physical mechanisms (blue curves marked with ' $L = 0$ ') and only the dark component (rose curves marked with ' $\Omega_b = 0$ '). Although dark energy is not dominant during the primordial times, these curves show its influence over the growth of the perturbations. However, this result was expected because different rates of vacuum decay means different quantities

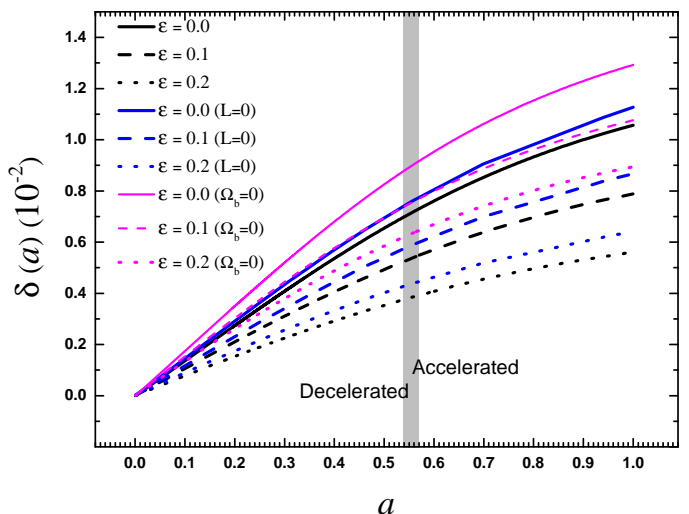


FIG. 3. Evolution of the density contrast of baryon and dark matter ($\delta(a) = \delta_b(a) + \delta_d(a)$) since the recombination until today ($a = 1$) for $\epsilon = 0, 0.1, 0.2$. Black curves specifies the models which take into account dark plus baryonic matter and the physical mechanisms; blue curves specifies those with dark matter plus baryonic matter without physical mechanisms; and rose curves specifies those with only dark component. The vertical band includes the redshift of transition of the three models. For this figure it was assumed $\Omega_{d0} = 0.229$, $\Omega_{b0} = 0.0458$ and $h = 0.702$.

of dark matter. Then, as bigger as the ϵ parameter, less is the dark matter quantity in early times. This delays the growth of the perturbations, making the amplitude of $\delta(a)$ to be smaller for bigger ϵ 's. This figure also shows the importance of the baryonic component as well the physical mechanisms taken together or alone. They delay the growth of the fluctuation. In the case with only baryonic matter without, the physical mechanisms is easy to see from equation (5), which shows that in case without baryonic matter the parameter $\tilde{\Omega}_{v0}$ is bigger (because the model is flat); and when the physical mechanisms are considered the main delay source is the cooling due to the formation of molecules. For a summary of this analysis see table III.

ϵ	Ω_{d0}	Ω_{b0}	Ω_{v0}	Cooling	$\delta_{d0} (10^{-2})$	$\delta_{b0} (10^{-2})$	$\delta_0 (10^{-2})$
0.0	0.229	0.0458	0.7252	yes	0.53	0.53	1.06
0.0	0.229	0.0458	0.7252	no	0.56	0.56	1.13
0.0	0.229	0	0.7710	-	0.65	0.65	1.29
0.1	0.229	0.0458	0.7252	yes	0.39	0.39	0.79
0.1	0.229	0.0458	0.7252	no	0.43	0.43	0.87
0.1	0.229	0	0.7710	-	0.54	0.54	1.08
0.2	0.229	0.0458	0.7252	yes	0.28	0.28	0.56
0.2	0.229	0.0458	0.7252	no	0.32	0.32	0.64
0.2	0.229	0	0.7710	-	0.45	0.45	0.89

TABLE III. Summary of the analysis about the figure 3 discussed in the text. The final density contrast (in $a = 1$) are δ_{d0} , δ_{b0} and $\delta_0 = \delta_{d0} + \delta_{b0}$ of the dark matter, baryonic matter and the total density contrast of the cloud.

The confidence levels result for the χ^2 minimization, from equation (6), are showed in figure 4 as black dashed curves. To delimit the degeneration of the space of parameters, the model (parameters $\Omega_{d0} - \epsilon$) was also compared with two more sets of observational data. One of them is the CMB-BAO ratio and the other is the cluster gas mass fraction from X-ray data, discussed in the following section.

IV. COMPLEMENTARY CONSTRAINTS

A. CMB-BAO ratio

As it is largely known, the CMB constrains from the so-called shift parameter \mathcal{R} [15] and the BAO measurement $A(z_{BAO})$ [16] have been commonly used to constrain non-standard models, but this approach is not completely correct since these quantities are derived by using parameters close to standard Λ CDM (see [17], [15], [18]).

In order to avoid some bias in our results we follow reference [17] and use the ratio CMB/BAO, i.e., $d_A(z_*)/D_V(z_{BAO})$ where z_* is the sound horizon at the last scattering. In fact, this is a product that cancels out some of the dependence on the sound horizon size at last scattering and a more model-independent constraint can be achieved in statistical analysis. Reference [17] gives this relation for the redshifts 0.2 and 0.35 (that come from the BAO in these redshifts) which were joined four more BAO data from 6dF Galaxy Survey Redshift (6dFGS) [31] and in the WiggleZ Dark Energy Survey [20]. These relations are presented in table IV. The χ^2 function to be minimized is

$$\chi_{CMB-BAO}^2 = \sum_{i=1}^6 \left(\frac{\left[\frac{d_A(z_*)}{D_V(z_{BAO,i})} \right]_{obs} - \left[\frac{d_A(z_*, \theta_i)}{D_V(z_{BAO,i}, \theta_i)} \right]_{th}}{\sigma_{CMB-BAO,i}} \right)^2, \quad (18)$$

where the theoretical ratio CMB-BAO is

$$\frac{d_A(z_*)}{D_V(z_{BAO})} = \frac{\int_0^{z_*} \frac{dz'}{E(z')}}{(1+z_*)} \left[\frac{E(z_{BAO})}{z_{BAO} \left(\int_0^{z_{BAO}} \frac{dz'}{E(z_{BAO})} \right)^2} \right]^{1/3}, \quad (19)$$

$z_* = 1090$ is the redshift assumed for the recombination, $E(z) = H(z)/H_0$ is given by equation (4), and z_{BAO} is the redshift of the BAO peaks (table IV).

The confidence levels are showed in figure 4 as dotted red curves.

Sample	z_{BAO}	$d_A(z_*)/D_V$
6dFGS	0.106	30.95 ± 1.50
2dFGRS	0.2	17.55 ± 0.65
SDSS	0.35	10.10 ± 0.38
WiggleZ	0.44	8.43 ± 0.67
WiggleZ	0.6	6.69 ± 0.33
WiggleZ	0.73	5.45 ± 0.31

TABLE IV. The observational CMB-BAO ratio data set.

B. Gas mass fraction constraint

For the other complementary observational comparison, we consider the data set of the baryonic content of 52 X-ray luminous galaxy clusters observed with Chandra in the redshift range $0.3 < z < 1.273$ provided by Ettori et al. [21].

Using equations (8) and (11) from [21], we have

$$f_{gas}^{model} = \frac{B\Omega_b}{[1.18 - 0.012kT_{gas}]\Omega_M} \quad (20)$$

where the depletion parameter $B = 0.874 \pm 0.0023$, the baryonic density parameter $\Omega_{b0} = 0.0458 \pm 0.0016$ and kT_{gas} is the gas temperature of each cluster.

However, the X-ray gas mass fraction values were determined for Λ CDM ($H_0, \Omega_M, \Omega_\Lambda$) = $(70 \text{ km s}^{-1} \text{ Mpc}^{-1})$, but since $f_{gas} \propto d_A^{3/2}$ (see [22]), the model function is defined by

$$f_{gas}^{model} = \frac{B\Omega_b}{[1.18 - 0.012kT_{gas}]\Omega_M} \left(\frac{d_A^{\Lambda CDM}}{d_A^{model}} \right)^{3/2}. \quad (21)$$

The distance ratio ($d_A^{\Lambda CDM}/d_A^{model}$) accounts for deviations in the geometry of the universe from the Λ CDM model, where

$$d_A^{\Lambda CDM} = \frac{c}{(1+z)H_{70}} \int_0^z \frac{dz}{\sqrt{0.3(1+z)^3 + 0.7}} \quad (22)$$

and

$$d_A^{model} = \frac{c}{(1+z)H_0} \int_0^z \frac{dz}{H(z)} \quad (23)$$

where $H(z)$ is the Hubble parameter of the model given by equation (4).

We find the constraints on the model parameters by minimizing the chi-squared function

$$\chi_{f_{gas}}^2 = \sum_{i=1}^{52} \frac{[f_{gas}^{model}(z_i, \theta_i) - f_{gas}^{obs}(z_i, \theta_i)]^2}{\sigma^2(i)_{f_{gas}^{model}} + \sigma^2(i)_{f_{gas}^{obs}}} \quad (24)$$

where $\sigma^2(i)_{f_{gas}^{model}}$ are the propagate errors, expressed by

$$\sigma(i)_{f_{gas}^{model}} = f_{gas}^{model} \sqrt{0.07 + \left(\frac{0.012kT(i)}{[1.18 - 0.012kT(i)]} \sigma(i)_{kT} \right)^2} \quad (25)$$

and $\sigma^2(i)_{f_{gas}^{obs}}$ are the errors for the Λ CDM data.

A similar analysis using gas mass fraction was done by first reference in [24], but they used the f_{gas} sample calculated in reference [23].

The confidence levels are showed in figure 4 as green dashed-dot curves. The joint analysis is given by

$$\chi_{joint}^2 = \chi_{gf}^2 + \chi_{CMB-BAO}^2 + \chi_{fgas}^2 \quad (26)$$

This analysis is showed in figure 4 as continuous blue curves.

Figure 4 shows that the regions representing the constraints from growth rate and gas mass fraction measurements on the parameter space $\Omega_{d0} - \epsilon$ are almost parallel, while the CMB-BAO measurements are approximately orthogonal to the last two measurements constraints. We also note that, notwithstanding the growth rate and gas mass fraction measurements come from different data sets, the first represents approximately the density contrast and the second the gas mass fraction in the cluster. This can mean that these data are measuring almost the same thing, which could explain why the confidence levels are parallel.

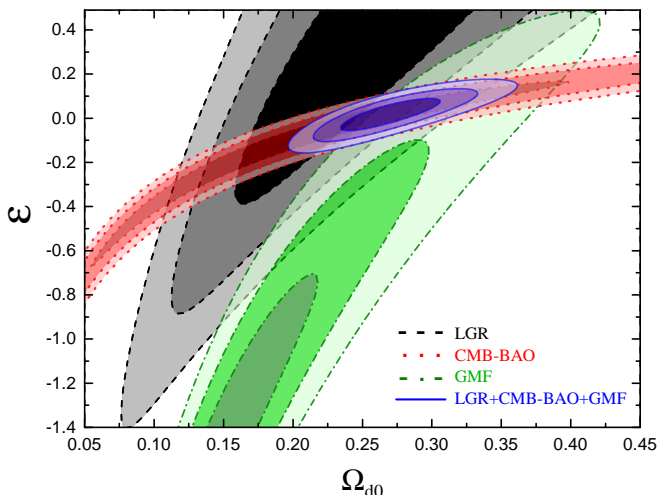


FIG. 4. Superposition of the confidence level contours of 68.3%, 95.4% and 99.73% in the $\Omega_{d0} - \epsilon$ plane from the linear growth rate (LGR), CMB-BAO ratio set (CMB-BAO) and the gas mass fraction (GMF), as well as their combination. The best fits and error bars are to 1σ ($\Delta\chi^2 = 1$) shown in table V.

The best fit values for each data set and for the joint analysis are presented in Table V.

Test	Ω_{d0}	ϵ	χ_{min}^2/ν
LGR	$0.254^{+0.054}_{-0.066}$	$0.35^{+0.13}_{-0.49}$	0.454
CMB-BAO	$0.193^{+0.125}_{-0.097}$	$-0.11^{+0.19}_{-0.30}$	0.815
GMF	$0.137^{+0.048}_{-0.036}$	$-1.68^{+0.64}_{-0.68}$	0.986
LGR+GMF+CMB-BAO	$0.269^{+0.023}_{-0.023}$	$0.02^{+0.04}_{-0.05}$	0.999

TABLE V. Limits to Ω_{d0} and ϵ with error bars standing for 1σ . LGR, CMB-BAO and GMF in the first column refer to Linear Growth Rate, Cosmic Microwave Background radiation - Baryon Acoustic Oscillations ratio and Gas Mass Fraction, respectively.

The results that we found are similar to that presented in references [7] and [24]. This mean that these results reinforces the conclusion already found by other authors about the possibility of a small, but measurable, deviation from the standard Λ dynamics (formally equivalent to the case $\epsilon = 0$).

V. CONCLUSIONS

In this paper we have studied the observational consequences of the decaying vacuum scenario proposed by Wang and Meng [6] considering the baryonic component, whose importance was pointed by Alcaniz and Lima [7], as well we have done one more slightly modification in the original model by considering the interaction between dark and baryonic matter components.

In order to enhance the importance of the baryonic component, two of the three analysis done was based in the observational data related with the baryonic mass, namely the ‘growth rate’ and ‘gas fraction in clusters of galaxies’. The third analysis was based in observational CMB-BAO rate, which proved to be a very useful complementary analysis because its confidence levels are transverse to the two first.

The theoretical counterpart of the growth rate was new and much more sophisticated than those we found in the literature. In this calculation, the baryonic and dark matter was considered as two fluids coupled and the main physical mechanisms present during and after recombination was also taken into account.

In conclusion, our statistical analysis reinforces the conclusion already found by others authors about the possibility of a small but measurable deviation from the standard Λ CDM.

ACKNOWLEDGMENTS

The author H. T. C. M. Souza is very grateful for the Brazilian agency CAPES. Also H. T. C. M. Souza is very grateful for the PDJ fellowship of the INCT IN-Espaço/CNPq for financial support. The author E. P. Bento is very grateful for the PNPd fellowship of the CAPES for financial support.

Appendix A: Temperature of the baryonic matter cloud

From recombination until the beginning of the collapse of the first structures, the baryonic matter (protons, electrons and hydrogen) can be treated as an ideal gas whose equation of state are given by

$$P = N_A k_B \rho_{cb} (1 + x_e) T_m, \quad (\text{A1})$$

where T_m is the temperature of the baryonic matter, k_B is the Boltzmann's constant, N_A the Avogadro's number, ρ_{cb} is the density of baryonic matter and the parameter x_e is the degree of ionization of the matter (in the beginning of the recombination $x_e = 1$). To simplify, in this work we have used the recombination given by [25], modified to include the collisional ionization among electrons and hydrogen atoms [26].

The energy equation is written as

$$\frac{dU}{dt} = -L + \frac{P}{\rho_{cb}^2} \frac{d\rho_{cb}}{dt}, \quad (\text{A2})$$

where U is the internal energy of the gas which is (per unit of mass m),

$$U = \frac{3}{2} N_A k_B T_m (1 + x_e), \quad (\text{A3})$$

and L is the cooling function which take into account the physical cooling/heating processes acting on the baryonic

matter, and it is given by

$$L = -k_B N_A T_m \frac{dx_e}{dt} - \frac{4k_B \sigma_T b T_\gamma^4 x_e}{m_p m_e c} (T_m - T_\gamma) + L_{H_2} + L_\alpha, \quad (\text{A4})$$

which includes recombination, photoionization and collisional ionization (first term), photon cooling (heating, second term), molecular hydrogen cooling and Lyman- α cooling (third and fourth terms, respectively). In this equation, m_p and m_e are the proton and electron masses, respectively; the speed of light is c , σ_T the Thomson cross section and $b = 4\sigma/c$, where σ is the Stefan-Boltzmann's constant. For more details about these terms see ref [27].

Using equations (A1) and (A3) into (A2), and $\rho_{cb} = \rho_{b0}(1 + \delta_b)$, we obtain the equation that governs the evolution of the temperature of the matter inside the cloud

$$\frac{dT_m}{dt} = -T_m \left[\frac{\dot{x}_e}{1 + x_e} + 2 \frac{\dot{a}}{a} - \frac{2}{3} \frac{\dot{\delta}_b}{1 + \delta_b} \right] - \frac{2}{3} \frac{L}{N_A k_B (1 + x_e)}. \quad (\text{A5})$$

The evolution of baryonic matter temperature of the Universe is the same equation (A5) disregarding the term with $\dot{\delta}_b$ (the last term in brackets).

For more details, the basic equations for the physical mechanisms were presented in various papers of de Araujo & Opher [28].

-
- [1] J. A. Frieman, *Lectures on Dark Energy and Cosmic Acceleration*, AIP Conf. Proc. **1057** (2008) 87 [arXiv:0904.1832].
- [2] S. Weinberg, *The cosmological constant problem*, *Rev. Mod. Phys.* **61** (1989) 1 [ADS]; P. J. Peebles and B. Ratra, *The cosmological constant and dark energy*, *Rev. Mod. Phys.* **75** (2003) 559 [arXiv:astro-ph/0207347]; T. Padmanabhan, *Cosmological constant-the weight of the vacuum*, *Phys. Rept.* **380** (2003) 235 [arXiv:hep-th/0212290]; J. A. S. Lima, *Alternative Dark Energy Models: An Overview*, *Braz. Journ. Phys.* **34** (2004) 194 [arXiv:astro-ph/0402109].
- [3] M. Ozer and M. O. Taha, *A possible solution to the main cosmological problems*, *PhLB* **171** (1986) 363 [ADS]; M. Ozer and M. O. Taha, *A model of the universe free of cosmological problems*, *NuPhB* **287** (1987) 776 [ADS]; O. Bertolami, *Time-dependence cosmological term*, *Nuovo Cimento B* **93** (1986) 36 [ADS]; K. Freese et al, *Cosmology with decaying vacuum energy*, *NuPhB* **287** (1987) 797 [ADS]; J. C. Carvalho, J. A. S. Lima and I. Waga, *Cosmological consequences of a time-dependent Λ term*, *Phys. Rev. D* **46** (1992) 2402 [ADS]; R. C. Arcuri and I. Waga, *Growth of density inhomogeneities in Newtonian cosmological models with variable Λ* , *Phys. Rev. D* **50** (1994) 2928 [ADS]; I. Waga, *Decaying vacuum flat cosmological models - Expressions for some observable quantities and their properties*, *ApJ* **414** (1993) 436 [ADS]; J. A. S. Lima and J. M. F. Maia, *Some Cosmological Consequences of a Λ -TERM Varying as $\beta H^2 + \alpha R^{-n}$* , *Mod. Phys. Lett. A* **8** (1993) 591 [ADS]; J. A. S. Lima and J. M. F. Maia, *Deflationary cosmology with decaying vacuum energy density*, *Phys. Rev. D* **49** (1994) 5597 [ADS]; J. A. S. Lima and M. Trodden, *Decaying vacuum energy and deflationary cosmology in open and closed universes*, *Phys. Rev. D* **53** (1996) 4280 [arXiv:astro-ph/9508049]; J. Salim and I. Waga, *Thermodynamic constraints on a time-dependent Lambda model (cosmology)*, *Class. Quant. Grav.* **10** (1993) 1767 [ADS]; A. I. Arbab, *Cosmological Models With Variable Cosmological and Gravitational "Constants" and Bulk Viscous Models*, *Gen. Rel. Grav.* **29** (1997) 61 [ADS]; J. M. Overduin and S. Cooperstock, *Evolution of the scale factor with a variable cosmological term*, *Phys. Rev. D* **58** (1998) 043506 [arXiv:astro-ph/9805260].
- [4] I. L. Shapiro and J. Solà, *Scaling behavior of the cosmological constant and the possible existence of new forces and new light degrees of freedom*, *Phys. Lett. B.* **475** (2000) 236 [arXiv:hep-ph/9910462]; J. V. Cunha, J. A. S. Lima and N. Pires, *Deflationary $\Lambda(t)$ cosmology: Observational expressions*, *A&A* **390** (2002) 809 [arXiv:astro-

- ph/0202217]; I. L. Shapiro and J. Solà, *The scaling evolution of the cosmological constant*, *J. High Energy. Phys.* **02** (2002) 006 [arXiv:hep-th/0012227]; J. S. Alcaniz and J. M. F. Maia, *Current and future supernova constraints on decaying Λ cosmologies*, *Phys. Rev. D.* **67** (2003) 043502 [arXiv:astro-ph/0212510]; R. Opher and A. Pelinsson, *Studying the decay of the vacuum energy with the observed density fluctuation spectrum*, *Phys. Rev. D.* **70** (2004) 063529 [arXiv:astro-ph/0405403]; Bauer F., *The running of the cosmological and the Newton constants controlled by the cosmological event horizon*, *Class. Quant. Grav.* **22** (2005) 3533 [arXiv:gr-qc/0501078]; S. Carneiro and J. A. S. Lima, *Time Dependent Cosmological Term and Holography*, *Int. J. Mod. Phys. A* **20** (2005) 2465 [arXiv:gr-qc/0405141]; J. D. Barrow and T. Clifton, *Cosmologies with energy exchange*, *Phys. Rev. D.* **73** (2006) 103520 [arXiv:gr-qc/0604063]; A. E. Montenegro Jr. and S. Carneiro, *Exact solutions of Brans Dicke cosmology with decaying vacuum density*, *Class. Quant. Grav.* **24** (2007) 313 [arXiv:gr-qc/0609059].
- [5] J. A. S. Lima, S. Basilakos and J. Solà, *Expansion History with Decaying Vacuum: A Complete Cosmological Scenario* (2013) 1 [arXiv:1209.2802 [gr-qc]].
- [6] P. Wang and X. Meng, *Can vacuum decay in our universe?*, *Class. Quantum Grav.* **22** (2005) 283 [arXiv:astro-ph/0408495].
- [7] J. S. Alcaniz and J. A. S. Lima, *Interpreting cosmological vacuum decay*, *Phys. Rev. D* **72** (2005) 063516 [arXiv:astro-ph/0507372].
- [8] P. J. E. Peebles, *The Large-Scale Structure of the Universe*, Princeton University Press (1980); P. J. E. Peebles, *The Peculiar Velocity Field in the Local Supercluster*, *ApJ* **205** (1976) 318 [ADS].
- [9] P. J. E. Peebles, *Principles of Physical Cosmology*, Princeton University Press (1993).
- [10] A. P. Lightman and P. L. Schechter, *The Omega dependence of peculiar velocities induced by spherical density perturbations*, *ApJ* **74** (1990) 831 [ADS].
- [11] R. Opher, N. Pires and J. C. N. de Araujo, *Growth of density perturbations with a cosmological constant*, *MNRAS* **285** (1997) 811 [ADS].
- [12] O. Lahav, P. B. Lilje, J. R. Primack, and M. J. Rees, *Dynamical effects of the cosmological constant*, *MNRAS* **251** (1991) 128 [ADS].
- [13] L. Wang and P. J. Steinhardt, *Cluster Abundance Constraints for Cosmological Models with a Time-varying, Spatially Inhomogeneous Energy Component with Negative Pressure*, *ApJ* **508** (1998) 483 [arXiv:astro-ph/9804015].
- [14] E. Komatsu et al., *Seven-year Wilkinson Microwave Anisotropy Probe (WMAP) Observations: Cosmological Interpretation*, *ApJS* **192** (2011) 1 [arXiv:1001.4538v3 [astro-ph]].
- [15] O. Elgaroy and T. Multamaki, *On using the cosmic microwave background shift parameter in tests of models of dark energy*, *A&A*, **471** (2007) 65 [arXiv:astro-ph/0702343].
- [16] D. J. Eisenstein et al, *Detection of the Baryon Acoustic Peak in the Large-Scale Correlation Function of SDSS Luminous Red Galaxies*, *ApJ* **633** (2005) 560 [arXiv:astro-ph/0501171].
- [17] J. Sollerman et al., *First-Year Sloan Digital Sky Survey-II (SDSS-II) Supernova Results: Constraints on Non-standard Cosmological Models*, *ApJ* **703** (2009) 1374 [arXiv:0908.4276 [astro-ph.CO]].
- [18] M. Doran, S. Stern and E. Thommes, *Baryon acoustic oscillations and dynamical dark energy*, *JCAP*, **04** (2007) 015
- [19] F. Beutler, *The 6dF Galaxy Survey: baryon acoustic oscillations and the local Hubble constant*, *MNRAS* **416** (2011) 3017 [arXiv:1106.3366 [astro-ph.CO]].
- [20] C. Blake, *The WiggleZ Dark Energy Survey: mapping the distance-redshift relation with baryon acoustic oscillations*, *MNRAS* **418** (2011) 1707 [arXiv:1108.2635 [astro-ph.CO]].
- [21] S. Ettori et al., *The cluster gas mass fraction as a cosmological probe: a revised study*, *A&A* **501** (2009) 61 [arXiv:0904.2740].
- [22] S. Sasaki, *A New Method to Estimate Cosmological Parameters Using the Baryon Fraction of Clusters of Galaxies*, *PASP*, **48** (1996) L119
- [23] S. W. Allen; D. A. Rapetti; R. W. Schmidt; H. Ebeling; R. G. Morris; A. C. Fabian, *Improved constraints on dark energy from Chandra X-ray observations of the largest relaxed galaxy clusters*, *MNRAS* **383** (2008) 879 [ADS]
- [24] R. S. Gonçalves, J. S. Alcaniz, A. Dev, and D. Jain, *Constraining dark matter-dark energy interaction with gas mass fraction in galaxy clusters*, *Mem. S.A.It.* **80** (2009) 921 [ADS]; F.E.M. Costa, J.S. Alcaniz, and J.M.F. Maia, *Coupled quintessence and vacuum decay*, *Phys. Rev. D* **77** (2008) 083516 [ADS] J. S. Alcaniz and J. A. S. Lima, *Interpreting cosmological vacuum decay*, *Phys. Rev. D* **72** (2005) 063516 [ADS]
- [25] P. J. E. Peebles, *Recombination of the Primeval Plasma*, *ApJ* **153** (1968) 1 [ADS].
- [26] R. J. Defouw, *Thermal Instability of a Model Hydrogen Plasma*, *ApJ* **161** (1970) 55 [ADS].
- [27] S.R. Oliveira, O.D. Miranda, J.C.N. de Araujo, R. Opher, *Collapse of primordial clouds - I*, *MNRAS* **301** (1998) 101 [arXiv:astro-ph/9808070].
- [28] J. C. N. de Araujo and R. Opher, *Collapse of population III objects*, *MNRAS* **231** (1988) 923 [ADS]; J. C. N. de Araujo and R. Opher, *The masses of Population III stars*, *MNRAS* **239** (1989) 371 [ADS]; J. C. N. de Araujo and R. Opher, *Formation of voids from negative density perturbations*, *ApJ* **350** (1990) 502 [ADS]; J. C. N. de Araujo and R. Opher, *Formation of galaxies in the early universe*, *ApJ* **437** (1994) 556 [ADS].
- [29] E. Hawkins et al., *The 2dF Galaxy Redshift Survey: correlation functions, peculiar velocities and the matter density of the Universe*, *MNRAS* **346** (2003) 78 [arXiv:astro-ph/0212375].
- [30] M. Davis et al., *Local gravity versus local velocity: solutions for β and non-linear bias*, *MNRAS* **413** (2011) 2906 [arXiv:1011.3114 [astro-ph.CO]].
- [31] F. Beutler et al., *The 6dF Galaxy Survey: $z \approx 0$ measurements of the growth rate and σ_8* , *MNRAS* **423** (2012) 3430 [arXiv:1204.4725 [astro-ph.CO]].
- [32] C. Blake et al., *The WiggleZ Dark Energy Survey: the growth rate of cosmic structure since redshift $z = 0.9$* , *MNRAS* **415** (2011) 2876 [arXiv:1104.2948[astro-ph.CO]].
- [33] A. Cabré and E. Gaztañaga, *Clustering of luminous red galaxies - I. Large-scale redshift-space distortions*, *MNRAS* **393** (2009) 1183 [arXiv:0807.2460 [astro-ph]].
- [34] M. Tegmark et al, *Cosmological constraints from the SDSS luminous red galaxies*, *PhRvD* **74** (2006) 123507 [arXiv:astro-ph/0608632].

- [35] C. Blake et al, *The WiggleZ Dark Energy Survey: the selection function and $z \approx 0.6$ galaxy power spectrum*, *MNRAS* **406** (2010) 803 [arXiv:1003.5721 [astro-ph.CO]].
- [36] E. V. Linder, *Cosmic Growth History and Expansion History*, *Phys. Rev. D* **72** (2005) 043529 [arXiv:astro-ph/0507263].
- [37] J. C. N. de Araujo and R. Opher, *Collapse of population III objects induced by cold collisionless dark matter*, *ApJ* **279** (1991) 461 [ADS].